

Giant effect of Sm atoms on time stability of (NdDy)(FeCo)B magnet

Roman B. Morgunov^{1,2,3}, Ekaterina I. Kunitsyna^{1,a}, Victor V. Kucheryaev², Vadim P. Piskorskii², Olga G. Ospennikova², and Eugene N. Kablov²

¹ Institute of Problems of Chemical Physics, Russian Academy of Sciences, Chernogolovka, 142432, Russia

² Institute of Aviation Materials, Moscow, 105005, Russia

³ Tambov State Technical University, Tambov, 392000, Russia

Received: 14 June 2016 / Revised: 2 September 2016

Published online: 30 September 2016 – © Società Italiana di Fisica / Springer-Verlag 2016

Abstract. Small amount of Sm additives ($\sim 1\text{--}3\text{ at.\%}$) slow down two times relaxation of magnetization of (NdDy)(FeCo)B alloys. Effective freezing of spontaneous relaxation of magnetization is caused by the enhancement of potential barriers of the domain walls. Easy plane single-ion anisotropy of Sm strongly disturbs the potential relief of the domain walls. The experimental results can be used to stabilize hard magnets.

1 Introduction

Relaxation of magnetization of solids has attracted the attention of specialists for a long time due to new fundamental regularities systematically discovered: tunneling of magnetization on high-spin molecules [1], elegant features of magnetic noise [2], and statistical regularities of domain walls motion [3]. All remagnetization phenomena are controlled by the height of the potential barrier separating magnetization states of different energies. Height of the remagnetization potential barrier both on high-spin molecules and in ferromagnetic crystals is controlled by single-ion anisotropy of magnetic ions [1]. The matter of potential relief of domain walls motion in the crystals composed of few ions of different single-ion symmetry of anisotropy has not been clarified so far. In the (NdDy)(FeCo)B alloy, Nd³⁺ and Dy³⁺ ions have “easy axis” symmetry in contrast to Sm³⁺ ion possessing “easy plane” symmetry (fig. 1).

One can expect the changes in local chaotically distributed obstacles as well as the changes in periodical Peierls relief under Sm doping. In the NdFeB structure, the lattice period is comparable with the domain wall width due to high magnetic anisotropy. According to [4,5] the Peierls relief strongly contributes to domain walls damping. In our paper a strong effect of the addition of a low concentration of Sm³⁺ ions to the (NdDy)(FeCo)B alloy on the dynamics of spontaneous demagnetization of the rare-earth magnets has been shown.

Another important problem our experiments were focused on is the stabilization of permanent magnet properties. The control over time relaxation and time stabilization of industrial magnets by small additives which would not disturb general magnetic properties is a key topic of modern research. Magnet quality is predetermined not only by widely mentioned characteristics formed immediately after magnet manufacturing (energy product, coercive force, saturation magnetization). The retention of these parameters for a long time at working temperature is of great importance. Stability of magnets is usually determined by spontaneous decrease of their magnetization recorded during 10⁴–10⁵ hours [5]. The disadvantages of this method are very long time of measurements and the necessity of increased temperature to accelerate demagnetization. Conclusion on time relaxation and magnetic viscosity obtained at high temperature one usually *a priori* generalizes to all temperatures implying the same physical mechanisms controlling time relaxation. Actually, relaxation dynamics is controlled not only by temperature and potential barrier relief. The spectrum of thermal fluctuation also significantly contributes to demagnetization. Thus, temperature increase can strongly change aging of the magnet. In this paper we used the method of sample demagnetization in reverse external magnetic field [6]. This technique allows one use few orders of magnitude shorter experimental time at the same temperature as it is necessary for magnet exploitation. At $T = 36\text{--}150\text{ K}$ magnetic hysteresis appears in sintered (Nd_{1-x}Sm_xDy)(FeCo)B magnets due to the reverse magnetic phase, while in the 150–350 K range domain walls

^a e-mail: kunya_kat@mail.ru

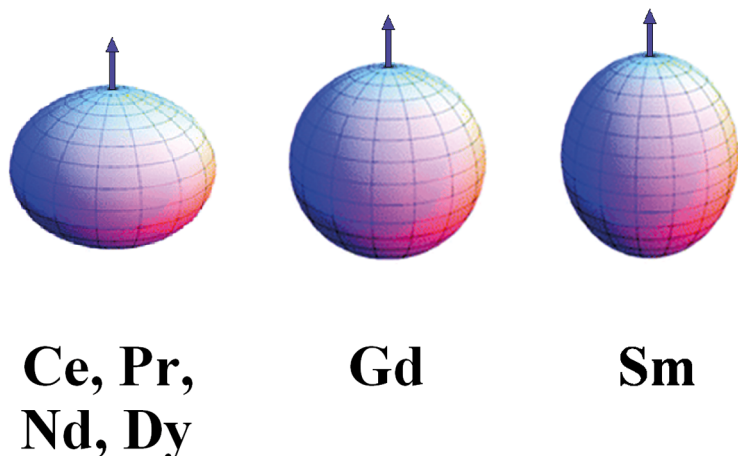


Fig. 1. Tensors of single-ion magnetic anisotropy of rare-earth ions contained in the studied alloys.

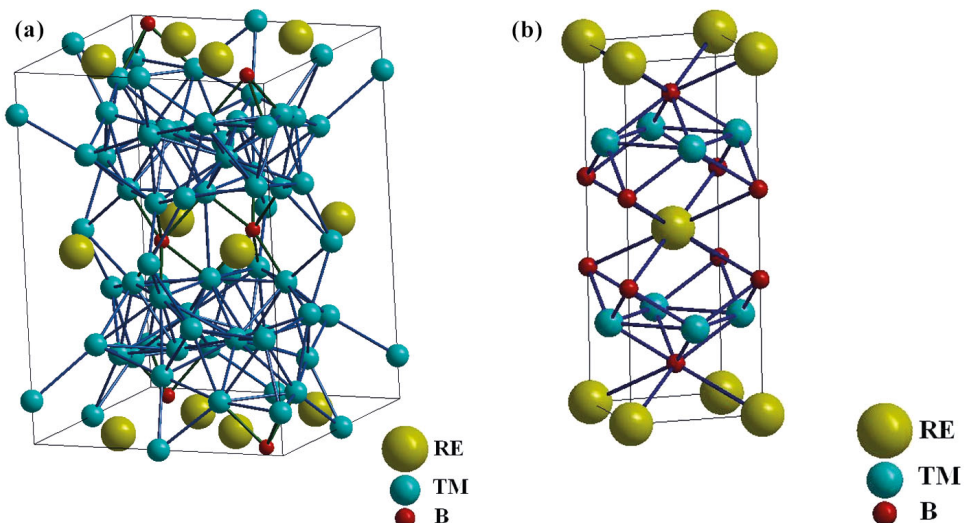


Fig. 2. Crystal structures of the 2-14-1 (a) and 1-2-2 (b) magnetic phases.

movement mainly contributes to magnetization dynamics [7]. Physical aspects of the rare-earth magnet stability are not discussed enough in the modern literature [8].

This work is aimed at the search for doping conditions of $(\text{Nd}_{1-x}\text{Sm}_x\text{Dy})(\text{FeCo})\text{B}$ magnet which stabilize magnetization to prevent its spontaneous relaxation and keep the rest magnetic properties undisturbed.

2 Experimental

The magnetically textured polysrystalline $(\text{Nd}_{0.67-x}\text{Dy}_{0.33}\text{Sm}_x)_{16.2}(\text{Fe}_{0.77}\text{Co}_{0.23})_{78.1}\text{B}_{5.7}$ samples were sintered in a 10^{-8} torr vacuum furnace. Typical grain sizes were $\sim 500 \pm 100 \mu\text{m}$. Accurate decription of the samples preparation as well as their phase analysis were presented in [7]. Contributions of the $(\text{NdDySm})_2(\text{FeCo})_{14}\text{B}$ (2-14-1) and $(\text{NdDySm})(\text{FeCo})_2\text{B}_2$ (1-2-2) phases, which crystal structures are presented in fig. 2 were $\sim 80\text{--}84\%$ and $\sim 16\text{--}20\%$, respectively. The total contribution of the rest 1-4-1 and 3-1 phases does not exceed 1%. Magnetic moments of the samples M were determined in constant magnetic field by MPMS SQUID 5XL Quantum design magnetometer 2–370 K temperatures in DC magnetic field up to 50 kOe.

Three series of plate-shaped samples $0.5 \times 2 \times 4 \text{ mm}^3$ in size with Sm concentrations $x = 0.05$ at.% (sample 1), $x = 0.18$ at. % (sample 2) and $x = 0$ at.% (sample 3) were compared in experiments. These x values correspond to 1–3% atomic concentration of Sm. Phase composition of 1, 2 and 3 samples are $(\text{Nd}_{0.62}\text{Dy}_{0.33}\text{Sm}_{0.05})_{16.2}(\text{Fe}_{0.77}\text{Co}_{0.23})_{78.1}\text{B}_{5.7}$, $(\text{Nd}_{0.49}\text{Dy}_{0.33}\text{Sm}_{0.18})_{16.2}(\text{Fe}_{0.77}\text{Co}_{0.23})_{78.1}\text{B}_{5.7}$, and $(\text{Nd}_{0.67}\text{Dy}_{0.33})_{16.2}(\text{Fe}_{0.77}\text{Co}_{0.23})_{78.1}\text{B}_{5.7}$, respectively. Before experiments samples were saturated in $H = 50 \text{ kOe}$ magnetic field until saturation magnetization M_S was reached. Repeting swithcing of the magnetic field (upper panel) were accompanied with mesurements of the $M(t)$ relaxation curves (bottom panel) at 300 (fig. 3). The magnetic response recorded at 300 K is shown in fig. 3.

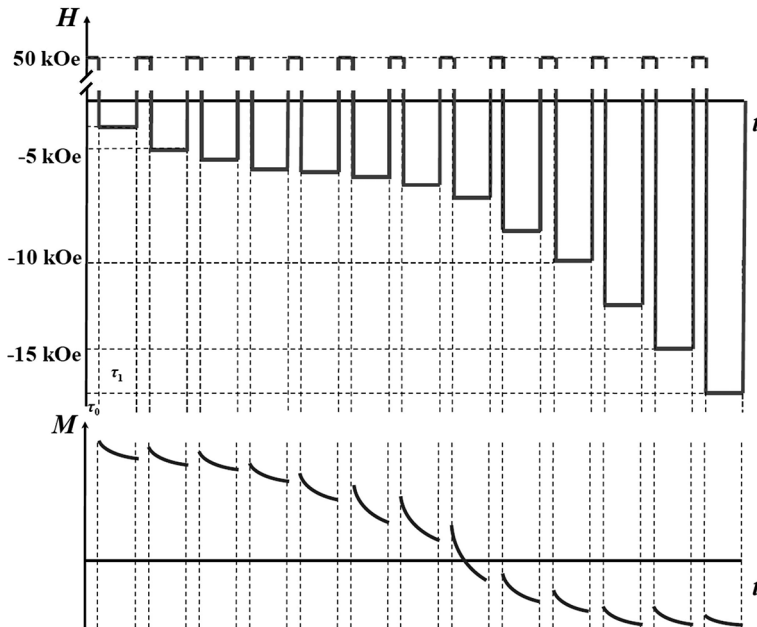


Fig. 3. Scheme of magnetic field switching (upper panel) and correspondent magnetization response (bottom panel).

3 Experimental results and discussion

The experimental dependences of magnetic moment change $\Delta M(t)$ recorded in different reverse magnetic fields at $T = 300\text{ K}$ are shown in semi-logarithmic coordinates in fig. 4. The dependence $\Delta M(t)$ follows the logarithmic law:

$$\frac{\Delta M}{M_S} \sim S \ln t. \quad (1)$$

Linearization of the $\Delta M(t)$ dependence in semi-logarithmic coordinates is shown in fig. 4. The tangent of the α slope of $\Delta M(\ln t)$ curve corresponds to magnetic viscosity $S = dM/d(\ln t)$. Logarithmic dynamics of demagnetization corresponds to a wide distribution of waiting time of depinning of domain walls from local obstacles. This mechanism and its competition with the nucleation of the reverse magnetic phase were discussed in [7].

Figure 4 shows the non-monotonous magnetic field dependence of $\Delta M(\ln t)$ slope and the corresponding dependence of magnetic viscosity $S(H)$. The field dependences of magnetic viscosity $S(H)$ for samples 1 (maximum at $H = 9\text{ kOe}$), 2 (maximum at $H = 2\text{ kOe}$) and 3 (maximum at $H = 9.5\text{ kOe}$) at 300 K are shown in fig. 5. A comparative analysis of the dependences in fig. 5 and fig. 6 allows us to conclude that the maxima of $S(H)$ dependences are close to corresponding coercive fields of the samples ($H_c = 9\text{ kOe}$ for sample 1, $H_c = 2\text{ kOe}$ for sample 2 and $H_c = 9.5\text{ kOe}$ for sample 3).

Analysis of the field dependence of magnetic viscosity requires standard normalization of viscosity assuming irreversible magnetic susceptibility χ_{irr} [9]:

$$S = S_V \chi_{irr}, \quad (2)$$

S_v is normalized viscosity independent of sample shape, χ_{irr} is irreversible magnetic susceptibility determined by formula [10]:

$$\chi_{irr} = \frac{\chi}{1 + N_\chi}, \quad (3)$$

$\chi = dM/dH$ is slope of the demagnetization curve (see fig. 6), N is demagnetization factor equal to 2.1 for samples 1, 2 and 3. The dependences $\chi(H)$ for samples 1, 2 and 3 are presented in fig. 7. These dependences were used to obtain dependences $\chi_{irr}(H)$ according to eq. (3).

The dependence of normalized viscosity was obtained by formula $S_v = S/\chi_{irr}(H)$. Generally, the field dependence of magnetic viscosity $S_v(H)$ can be determined by the following equation [11]:

$$S_V = -\frac{K_B T}{\left(\frac{\partial E}{\partial H}\right)_T}, \quad (4)$$

k_B is the Boltzmann constant, E is the activation energy of domain wall unpinning. The shape of the $S_v(H)$ dependence is controlled by the mechanism of domain walls pinning. In case of “weak” pinning activation energy can be expressed

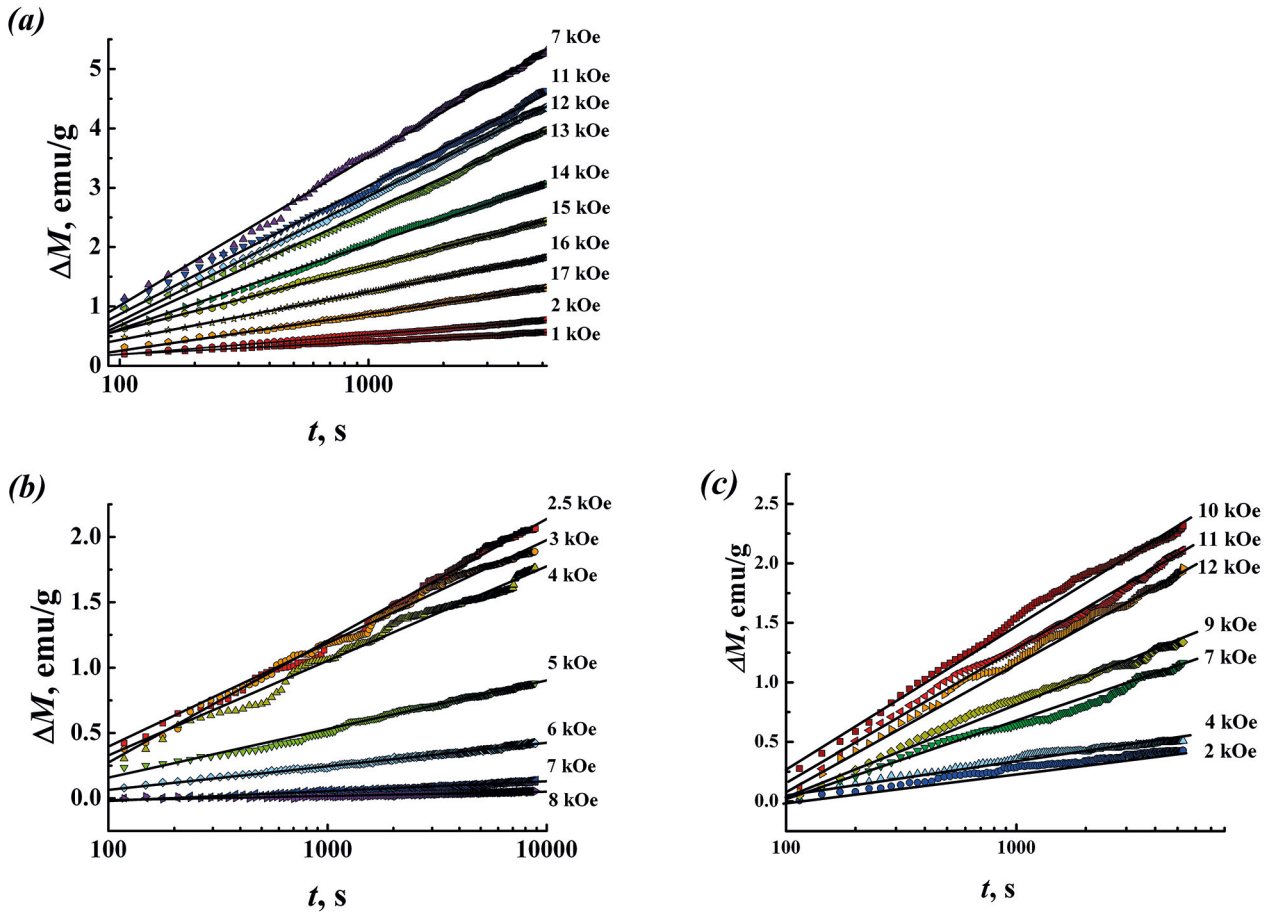


Fig. 4. Time dependences of magnetic moment variation $\Delta M(t)$ in different magnetic fields recorded at $T = 300$ K for samples 1 (a), 2 (b), 3 (c). Approximation is shown by solid lines.

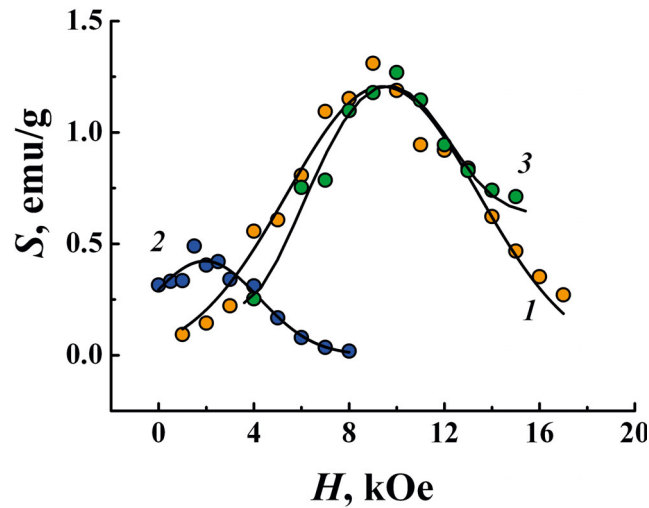


Fig. 5. Dependences of magnetic viscosity S on magnetic field H at $T = 300$ K in samples 1, 2 and 3. Approximation is shown by solid lines.

by formula [11]:

$$E = 31\gamma b^2 \left(1 - \frac{H}{H_0}\right), \quad (5)$$

γ is the surface energy density of domain wall, $4b$ is the thickness of domain wall, H_0 is the threshold magnetic field of the domain wall depinning in the absence of thermal activation. In case of “strong” pinning activation energy should

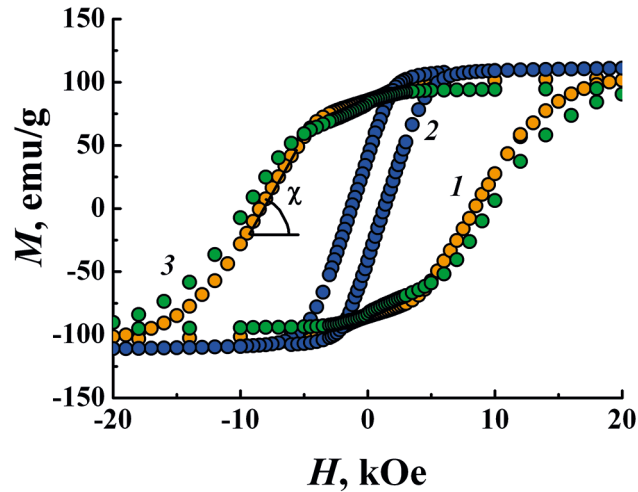


Fig. 6. Hysteresis loops of samples 1, 2 and 3 at $T = 300\text{ K}$. Magnetic field is directed along the easy axis.

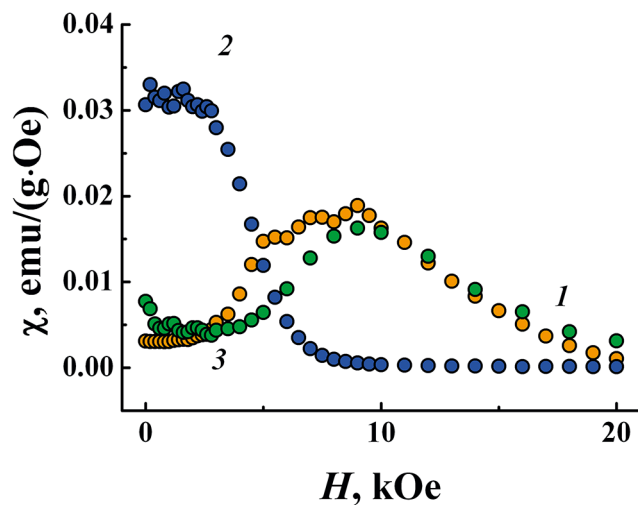


Fig. 7. Dependences of magnetic susceptibility $\chi = dM/dH$ on magnetic field at $T = 300\text{ K}$ for samples 1, 2 and 3.

be expressed as [12]

$$E = \frac{4fb}{3} \left[1 - \left(\frac{H}{H_0} \right)^{1/2} \right]^{3/2}, \quad (6)$$

f is the force providing single depinning of the domain wall. The above-mentioned cases of weak and strong pinning are differentiated by the parameter $\beta = 3f/(8\pi\gamma b)$: at $\beta < 1$, weak pinning takes place, while at $\beta > 1$ the model of strong pinning should be used.

Shape of the $S_V(H)$ curve allows us to distinguish which case is realized in our alloys. The substitution of eq. (5) to (4) results in the field-independent viscosity $S_v = k_B TH_0/31\gamma b^2$ that is in contradiction with the experimental data (fig. 6). The substitution of eq. (6) to (4), results in the field-dependent expression for magnetic viscosity:

$$S_V = \frac{k_B T}{fb} \frac{[H \cdot H_0]^{1/2}}{\left[1 - \left(\frac{H}{H_0} \right)^{1/2} \right]^{1/2}}. \quad (7)$$

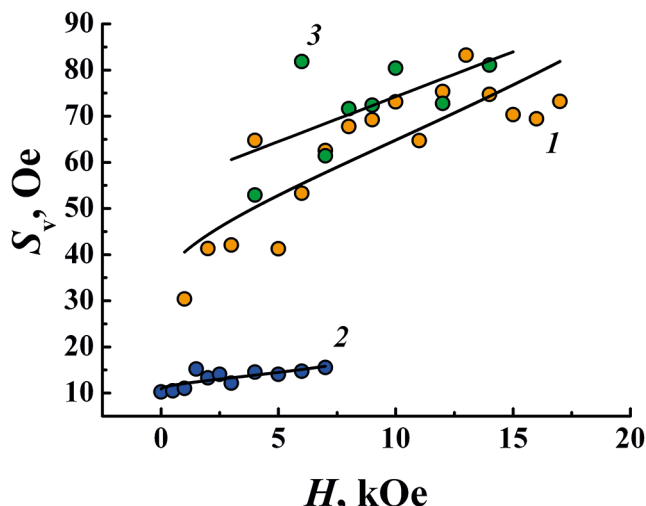


Fig. 8. Dependences of normalized magnetic viscosity S_v on magnetic field recorded for samples 1, 2 and 3 at $T = 300\text{ K}$. Approximations are shown by solid lines.

Solid lines in fig. 8 are approximations of the $S(H)$ dependences by eq. (7). The approximation resulted in $fb = 4 \cdot 10^{-11} \text{ erg}$ for sample 1, $fb = 2 \cdot 10^{-10} \text{ erg}$ for sample 2 and $fb = 3 \cdot 10^{-11} \text{ erg}$ for sample 3. The obtained values are in the range typical for $\text{Nd}_2\text{Fe}_{14}\text{B}$ magnets [9]. Parameter fb is mechanical work necessary to overcome domain wall obstacle under magnetic field application. A fivefold difference in parameter fb for samples 1 and 2, which show very small difference in compositions and Sm concentrations means a huge positive effect of Sm on time stability of the magnet.

4 Conclusion

Giant deceleration of magnetization relaxation caused by the addition of small amount of Sm ($\sim 1\text{--}3\%$) was found in the $(\text{NdDy})(\text{FeCo})\text{B}$ rare-earth magnet. “Easy plane” magnetic anisotropy of Sm ion disturbs “easy axis” Nd and Dy single-ion anisotropy and strongly modifies potential relief of domain walls as well as energy necessary for unpinning. Sm additive can be used to stabilize effectively the rare-earth hard magnet properties.

References

1. D. Gatteschi, R. Sessoli, Angew. Chem. Int. Ed. **42**, 268 (2003).
2. J. Brooke, T.F. Rosenbaum, G. Aeppli, Nature **413**, 610 (2001).
3. L. Neel, J. Phys. Radium **11**, 49 (1950).
4. E.P. Wohlfarth, J. Phys. F **14**, 2155 (1984).
5. R.W. Chantrell, A. Lyberatos, E.P. Wohlfarth, J. Phys. F **16**, L145 (1986).
6. L. Wang, J. Ding, Y. Li, Y.P. Feng, X.Z. Wang, J. Magn. & Magn. Mater. **206**, 127 (1999).
7. E. Kablov, O. Ospennikova, V. Piskorskii, D. Korolev, A. Dmitriev, E. Kunitsyna, R. Morgunov, Eur. Phys. J. Plus **131**, 40 (2016).
8. J.F. Herbst, Rev. Mod. Phys. **63**, 819 (1991).
9. D. Givord, P. Tenaud, T. Viadieu, G. Hadjipanayis, J. Appl. Phys. **61**, 3454 (1987).
10. C.K. Mylvaganam, P. Gaunt, Philos. Mag. B **44**, 581 (1981).
11. P. Gaunt, Philos. Mag. B **48**, 261 (1983).
12. E.N. Kablov, V.P. Piskorskii, R.A. Valeev, O.G. Ospennikova, I.I. Rezhikova, N.S. Moiseeva, Russ. Metall. (Metally) **7**, 547 (2014).